

Cleaning graphene with a titanium sacrificial layer

C. A. Joiner, T. Roy, Z. R. Hesabi, B. Chakrabarti, and E. M. Vogel

Citation: [Applied Physics Letters](#) **104**, 223109 (2014); doi: 10.1063/1.4881886

View online: <http://dx.doi.org/10.1063/1.4881886>

View Table of Contents: <http://scitation.aip.org/content/aip/journal/apl/104/22?ver=pdfcov>

Published by the [AIP Publishing](#)

Articles you may be interested in

[Cyclododecane as support material for clean and facile transfer of large-area few-layer graphene](#)

Appl. Phys. Lett. **105**, 113101 (2014); 10.1063/1.4895733

[Direct growth of graphene on Si\(111\)](#)

J. Appl. Phys. **115**, 223704 (2014); 10.1063/1.4882181

[Optimization of HfO₂ films for high transconductance back gated graphene transistors](#)

Appl. Phys. Lett. **103**, 073105 (2013); 10.1063/1.4818467

[Few layer graphene synthesized by filtered cathodic vacuum arc technique](#)

J. Vac. Sci. Technol. B **31**, 040602 (2013); 10.1116/1.4813762

[Local solid phase growth of few-layer graphene on silicon carbide from nickel silicide supersaturated with carbon](#)

J. Appl. Phys. **113**, 114309 (2013); 10.1063/1.4795501



Cleaning graphene with a titanium sacrificial layer

C. A. Joiner,^{1,a)} T. Roy,¹ Z. R. Hesabi,¹ B. Chakrabarti,^{1,2} and E. M. Vogel¹

¹*School of Materials Science and Engineering, Georgia Institute of Technology, Atlanta, Georgia 30332, USA*

²*Department of Materials Science and Engineering, The University of Texas at Dallas, Richardson, Texas 75080, USA*

(Received 25 February 2014; accepted 26 May 2014; published online 4 June 2014)

Graphene is a promising material for future electronic applications and chemical vapor deposition of graphene on copper is a promising method for synthesizing graphene on the wafer scale. The processing of such graphene films into electronic devices introduces a variety of contaminants which can be difficult to remove. An approach to cleaning residues from the graphene channel is presented in which a thin layer of titanium is deposited via thermal e-beam evaporation and immediately removed. This procedure does not damage the graphene as evidenced by Raman spectroscopy, greatly enhances the electrical performance of the fabricated graphene field effect transistors, and completely removes the chemical residues from the surface of the graphene channel as evidenced by x-ray photoelectron spectroscopy. © 2014 AIP Publishing LLC. [<http://dx.doi.org/10.1063/1.4881886>]

Graphene grown on copper via chemical vapor deposition (CVD) is a promising candidate for the fabrication of graphene based devices on a large scale.¹ One key issue preventing graphene from being fully integrated into conventional complementary metal oxide semiconductor (CMOS) processing is the sensitivity of graphene to processing conditions.^{2–5} The transfer of CVD grown graphene and the conventional photolithography processes used in the fabrication of graphene devices have been shown to leave behind residue negatively impacting device performance.⁶ To date, several techniques for the cleaning of graphene such as thermal annealing,⁷ electrical current annealing,⁸ plasma cleaning,⁹ and chloroform treatments¹⁰ have been used with varying degrees of success. While high temperature annealing under a high vacuum environment has been shown to completely remove residues from the graphene surface,¹¹ there is concern that annealing for extended periods may result in degradation of the metal contacts as well as the creation of free radicals from polymer scission which may react with graphene defects as well as making the graphene surface more susceptible to doping from the environment.^{12,13} Electrical current annealing has been shown to be an effective means for cleaning individual graphene devices, but has shown limited success in removing residues from large graphene areas. Plasma cleaning processes reported in the literature involve highly reactive oxygen and hydrogen species as well as ion bombardment which results in defect generation in the graphene sheets.^{14,15} Chloroform cleaning treatments are not desirable due to its toxicity. Therefore, other methods for the removal of residues introduced during processing are needed in order to fully incorporate graphene into traditional CMOS processing. In this study, we report the use of a sacrificial Ti layer to remove residues from the graphene surface.

CVD graphene on copper purchased from ACS Material, www.acsmaterial.com, was used in this study. The wet transfer process presented in Ref. 11 was used to transfer

the graphene from the copper to a Si/SiO₂ substrate (90 nm thermal oxide). Back gated field effect transistors (FETs) were fabricated using conventional photolithography and e-beam evaporation for the deposition of Ni contacts capped with Au. Three sets of devices (15 devices per set) were fabricated using graphene from the same copper foil (i.e., graphene grown during the same run) and transferred to a substrate cleaved from the same Si/SiO₂ wafer to prevent run-to-run variations in the data. The first set of devices, labeled “as-is,” did not receive any post fabrication treatments following device fabrication. The second set of devices, labeled “HF-cleaned,” was treated with a 200:1 DI:HF solution for 30 s. The third set of devices, labeled “Ti-cleaned,” had 2 nm of Ti deposited via e-beam evaporation at a rate of 1 Å/s and was subsequently etched using a 200:1 DI:HF solution until the Ti was completely removed as evidenced by x-ray photoelectron spectroscopy (XPS). The thickness of 2 nm was chosen as the thickness was sufficient to provide complete coverage of the graphene and did not require a significant etch time to remove. Thicker depositions are not expected to impact the cleaning procedure other than increasing the etch time required to fully remove the Ti layer. The deposition rate was chosen due to system calibration settings and is not expected to significantly impact the cleaning procedure. All electrical measurements were carried out in a Lakeshore cryogenic probe station under vacuum (5×10^{-6} Torr) following an overnight 80 °C *in situ* anneal in order to remove environmental adsorbates from the graphene channel.¹¹

Figure 1 shows a summary of the electrical characterization of the prepared devices. The mobility, intrinsic or impurity carrier concentration, and minimum conductance point were extracted from the $I_d - V_g$ curves using a method outlined elsewhere.^{16,17} The mobility, impurity carrier concentration, and minimum conductance point can give a clear indication in the amount of contamination on the graphene channel. Contamination on the graphene channel acts as scattering centers for the charge carriers, decreasing the mobility due to increased scattering. Contamination on the

^{a)}Author to whom correspondence should be addressed. Electronic mail: cjoiner3@gatech.edu

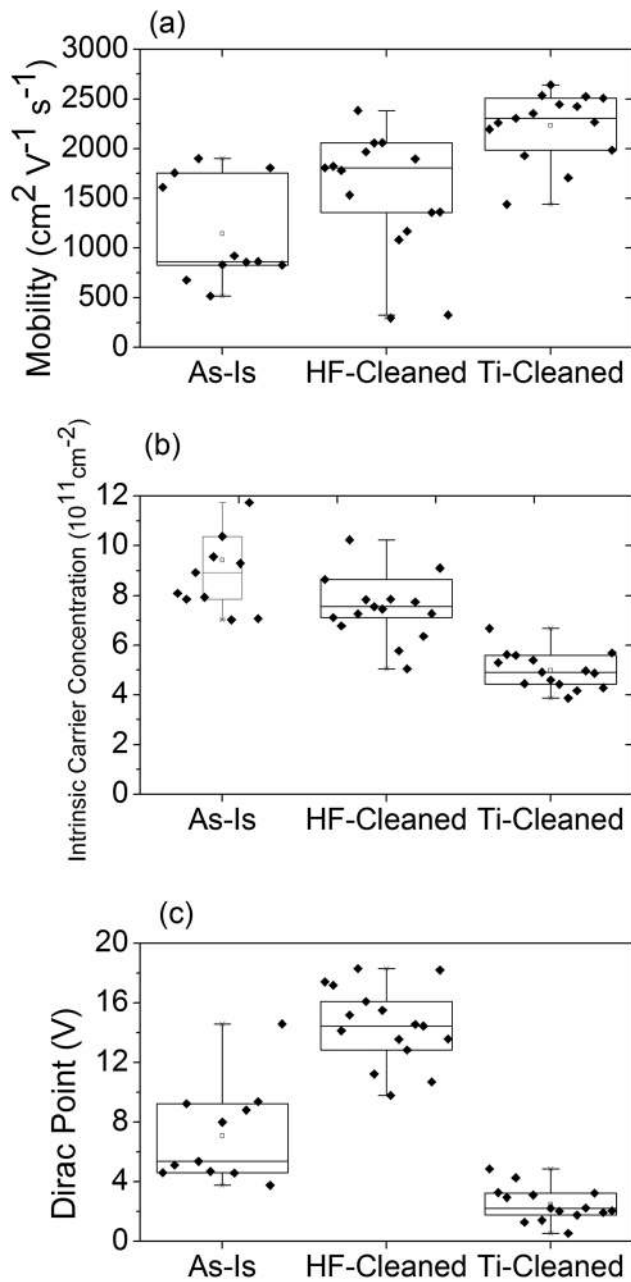


FIG. 1. (a) Mobility measurements of the as-is, HF-cleaned, and Ti-cleaned devices. Ti cleaning results in the highest mobility. (b) Intrinsic or impurity carrier concentration measurements. The Ti cleaning results in a significant improvement. (c) Minimum conductance point measurements. The Ti-Clean devices shift towards the intrinsic point of graphene while the HF cleaning shifts away from the intrinsic point of 0 V.

surface can also act as dopants, injecting additional charge carriers into the graphene channel resulting in a rise of the impurity carrier concentration. The minimum conductance point of the graphene can be impacted by the introduction of charge inhomogeneity from the contamination in the form of electron/hole puddles or charged contamination species. Figure 1(a) shows the mobility of the devices. The as-is devices have an average mobility of $1142 \text{ cm}^2 \text{V}^{-1} \text{s}^{-1}$. The HF-cleaned devices saw an increase in average mobility up to $1806 \text{ cm}^2 \text{V}^{-1} \text{s}^{-1}$ suggesting partial removal of the contamination, while the Ti-cleaned devices showed the largest average mobility of $2235 \text{ cm}^2 \text{V}^{-1} \text{s}^{-1}$. From Figure 1(b), the impurity carrier concentration is slightly reduced

following the HF cleaning, but is not as effective as the Ti removal process which reduces the impurity carrier concentration from $9.41 \times 10^{11} \text{ cm}^{-2}$ to $4.98 \times 10^{11} \text{ cm}^{-2}$. Figure 1(c) shows the minimum conductance point of the graphene devices. The as-is samples have an average minimum conductance point of 7.09 V. The HF cleaned samples show an increase in the minimum conductance point to 14.4 V, suggesting an increase in charge inhomogeneity on the graphene surface possibly due to the addition of fluorine or hydrogen to the graphene or due to changes in the underlying substrate resulting from HF exposure. The Ti cleaning procedure results in the minimum conductance point moving to 2.48 V, closer to the intrinsic minimum conductance point of 0 V for graphene indicating a removal of contamination from the channel.

The impact of the cleaning procedures on the graphene was characterized using Raman spectroscopy. The Raman characterization was performed in a Thermo Scientific Nicolet Almega XR using an excitation wavelength of 488 nm. As can be seen in Figure 2(a), the D-band is similar for graphene from all three processes, signifying that the e-beam evaporation of Ti and the chemical etching process do not damage the graphene. The G band position shifts from 1582 cm^{-1} to 1572 cm^{-1} after Ti deposition as seen in Figure 2(b), suggesting that the metal deposition causes doping in the channel.¹⁸ Figure 2(b) also shows that following the removal of Ti from

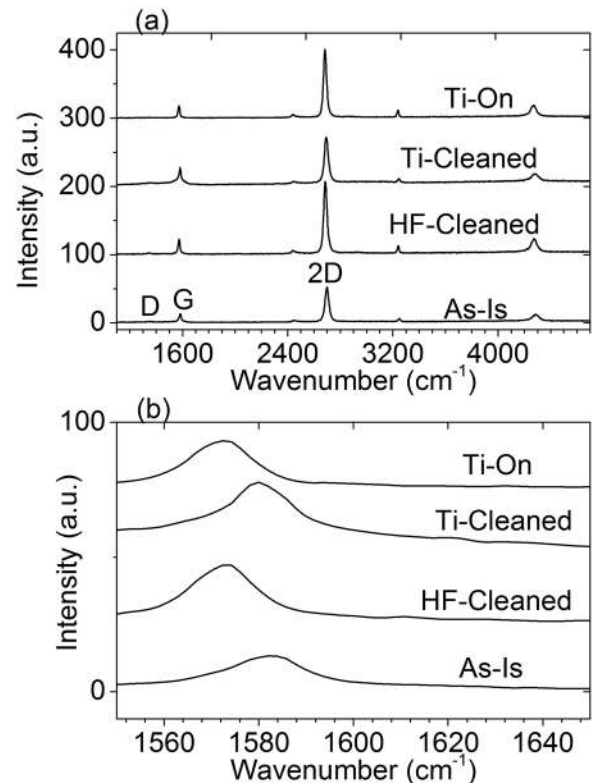


FIG. 2. (a) The Raman spectra for the as-is, HF-cleaned, and Ti-Cleaned samples (both before and after Ti removal). For all samples, the 2D/G ratio is greater than 2:1 indicating monolayer samples. The D peak is negligible in all four spectrums indicating no damage occurs to the graphene during the processing of the devices or during the cleaning procedure. The 2D, G, and D peak positions are labeled with their respective letter designations. (b) The G peak of the as-is, HF-cleaned, and Ti-cleaned samples. Shifting in the spectrum signifies doping, with Ti-cleaning being the closest to the intrinsic position of 1580 cm^{-1} .

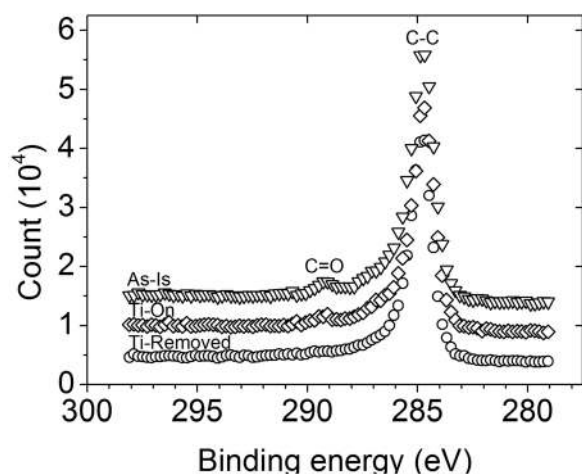


FIG. 3. The C1s XPS spectra of the as-is, Ti-On, and Ti-removed samples (triangles, diamonds, and circles, respectively). The C=O peak located at 289 eV is completely removed following the Ti etching indicating complete removal of the PMMA.

the channel, the G band position shifts to a value of 1580 cm^{-1} .¹⁹ This indicates that the dopants associated with the Ti deposition do not remain after Ti removal and that Raman can be used as a simple and effective means to determine if all Ti has been removed. Interestingly, the Raman spectrum of the HF cleaned sample shows significant doping as seen in Figure 2(b), and further indicates that HF alone is not an effective means to clean graphene as it introduces doping into the channel. This is not present in the Ti-cleaned sample despite over etching to ensure all Ti is removed.

Following the Raman and electrical characterization, the HF cleaning procedure was deemed to be inferior to the Ti cleaning process due to the apparent doping associated with the process and non-ideal electrical characterization. To further characterize the effectiveness of the Ti cleaning procedure, an XPS analysis was performed on the as-is and Ti-cleaned samples. The C1s XPS spectrum of poly(methyl methacrylate) (PMMA) has peaks at 289.03, 286.90, 285.68, 285.00 eV in a 1:1:1:2 ratio corresponding to the carbon-oxygen double bond, carbon-oxygen single bond, quaternary carbon bonds, and secondary/tertiary carbon bonds, respectively.²⁰ As can be seen in Figure 3, the as-is sample has an easily distinguishable peak located at 289 eV. This peak was used as a signature of the presence of PMMA due to the absence of such a peak in pristine graphene spectrums and because the peak is easily distinguishable from the main carbon peak at 285 eV.²¹ The Ti deposited spectrum clearly shows a peak at 289 eV, indicating the PMMA is still present following the Ti deposition. Following the Ti removal, the peak at 289 eV is completely removed, indicating the complete removal of PMMA residues from the graphene channel. The Ti deposition results in Ti bonding with the oxygen sites in the oxygen rich PMMA residue as evidenced by the Ti 2p spectra (not shown) containing peaks at 458 and 464 eV, consistent with complete oxidation of the Ti layer, as well as the absence of the Ti-C peak at 282.7 eV in the C1s spectra. This bonding with the oxygen species in the PMMA assists in the breakdown of the PMMA residue, allowing the residues to be easily removed via HF removal of the Ti layer.

In conclusion, the Ti cleaning process as outlined here is a CMOS compatible method for removing residues from

graphene that are associated with transfer and device fabrication. This Ti cleaning process results in a substantial improvement of mobility, a large reduction in the minimum conductance point and removal of dopants as evidenced by the decrease in intrinsic carrier concentration as well as the G band of the Raman spectrum shifting to the intrinsic value of 1580 cm^{-1} . The XPS spectrum indicates the complete removal of PMMA residues to within the level of XPS sensitivity. The Raman spectrum further shows that the Ti cleaning process does not damage the graphene channel, as the D peak did not increase from the as-is to the Ti-cleaned sample. We have further demonstrated that the deposition and removal of the titanium layer is a necessary step as HF alone results in significant doping of the graphene channel. We have thus shown our Ti cleaning process to be a simple and effective method of cleaning the graphene layer without the drawbacks associated with other cleaning methods.

This work was supported in part by the Center for Low Energy Systems Technology (LEAST), one of six centers supported by the STARnet phase of the Focus Center Research Program (FCRP), a Semiconductor Research Corporation program sponsored by MARCO and DARPA. This work was also supported by funding from the NSF MRSEC: The Georgia Tech Laboratory for New Electronic Materials (Award No. 0820382).

- ¹X. S. Li, W. W. Cai, J. H. An, S. Kim, J. Nah, D. X. Yang, R. Piner, A. Velamakanni, I. Jung, E. Tutuc, S. K. Banerjee, L. Colombo, and R. S. Ruoff, *Science* **324**(5932), 1312 (2009).
- ²F. Schedin, A. K. Geim, S. V. Morozov, E. W. Hill, P. Blake, M. I. Katsnelson, and K. S. Novoselov, *Nature Mater.* **6**(9), 652 (2007).
- ³B. Huang, Z. Y. Li, Z. R. Liu, G. Zhou, S. G. Hao, J. Wu, B. L. Gu, and W. H. Duan, *J. Phys. Chem. C* **112**(35), 13442 (2008).
- ⁴H. J. Yoon, D. H. Jun, J. H. Yang, Z. X. Zhou, S. S. Yang, and M. M. C. Cheng, *Sens. Actuators, B* **157**(1), 310 (2011).
- ⁵C. W. Chen, F. Ren, G. C. Chi, S. C. Hung, Y. P. Huang, J. Kim, I. Kravchenko, and S. J. Pearton, *J. Vac. Sci. Technol., B* **30**(4), 040602 (2012).
- ⁶M. Her, R. Beams, and L. Novotny, *Phys. Lett. A* **377**(21–22), 1455 (2013).
- ⁷Z. H. Ni, H. M. Wang, Z. Q. Luo, Y. Y. Wang, T. Yu, Y. H. Wu, and Z. X. Shen, *J. Raman Spectrosc.* **41**(5), 479 (2010).
- ⁸J. Moser, A. Barreiro, and A. Bachtold, *Appl. Phys. Lett.* **91**(16), 163513 (2007).
- ⁹Y. D. Lim, D. Y. Lee, T. Z. Shen, C. H. Ra, J. Y. Choi, and W. J. Yoo, *ACS Nano* **6**(5), 4410 (2012).
- ¹⁰Z. G. Cheng, Q. Y. Zhou, C. X. Wang, Q. A. Li, C. Wang, and Y. Fang, *Nano Lett.* **11**(2), 767 (2011).
- ¹¹J. Chan, A. Venugopal, A. Pirkle, S. McDonnell, D. Hinojos, C. W. Magnuson, R. S. Ruoff, L. Colombo, R. M. Wallace, and E. M. Vogel, *ACS Nano* **6**(4), 3224 (2012).
- ¹²Y. C. Lin, C. C. Lu, C. H. Yeh, C. H. Jin, K. Suenaga, and P. W. Chiu, *Nano Lett.* **12**(1), 414 (2012).
- ¹³H. Sojoudi, J. Baltazar, C. Henderson, and S. Graham, *J. Vac. Sci. Technol., B* **30**(4), 041213 (2012).
- ¹⁴D. C. Kim, D. Y. Jeon, H. J. Chung, Y. Woo, J. K. Shin, and S. Seo, *Nanotechnology* **20**(37), 375703 (2009).
- ¹⁵I. Childres, L. A. Jauregui, J. F. Tian, and Y. P. Chen, *New J. Phys.* **13**, 025008 (2011).
- ¹⁶S. Kim, J. Nah, I. Jo, D. Shahrjerdi, L. Colombo, Z. Yao, E. Tutuc, and S. K. Banerjee, *Appl. Phys. Lett.* **94**(6), 062107 (2009).
- ¹⁷A. Venugopal, J. Chan, X. S. Li, C. W. Magnuson, W. P. Kirk, L. Colombo, R. S. Ruoff, and E. M. Vogel, *J. Appl. Phys.* **109**(10), 104511 (2011).
- ¹⁸A. C. Ferrari and D. M. Basko, *Nat. Nanotechnol.* **8**(4), 235 (2013).
- ¹⁹A. C. Ferrari, *Solid State Commun.* **143**(1–2), 47 (2007).
- ²⁰G. Beamsom, A. Bunn, and D. Briggs, *Surf. Interface Anal.* **17**(2), 105 (1991).
- ²¹A. Pirkle, J. Chan, A. Venugopal, D. Hinojos, C. W. Magnuson, S. McDonnell, L. Colombo, E. M. Vogel, R. S. Ruoff, and R. M. Wallace, *Appl. Phys. Lett.* **99**(12), 122108 (2011).